Chapter 9

Optical Diode Based on Two-Dimensional Photonic Crystal

Han Ye, Yumin Liu and Zhongyuan Yu

Additional information is available at the end of the chapter

http://dx.doi.org/10.5772/intechopen.71053

Abstract

The integrated optical diodes have been a thriving research theme due to their potential on-chip applications in photonic circuits for all-optical computing and information processing. Analogous to electronic counterparts, the unidirectional light propagation is characterized by the high contrast between forward and backward transmissions. In this chapter, we demonstrate the proposed schemes and designs for reciprocal and nonreciprocal optical diodes based on two-dimensional (2D) photonic crystal (PhC). The reciprocal devices are built by linear and passive PhC, and the spatial asymmetric mode conversion is utilized to achieve the unidirectionality. The presented nonreciprocal optical diodes rely on the optical nonlinearity of cavity. New 2D PhC optical diodes with high contrast ratio, low insertion loss, large operational bandwidth, small device footprint, and ease of fabrication are highly desirable and still pursued.

Keywords: two-dimensional photonic crystal, optical diode, unidirectional transmission, time-reversal symmetry, mode conversion, nonlinear effect

1. Introduction

The optical diodes, as the counterpart of electron diodes in optics, have attracted huge interests due to its capability of asymmetric light propagation. The unidirectionality invokes potential applications in integrated optical circuits for all-optical computing and information processing [1–5]. Highly desirable key performances of an optical diode are high contrast ratio, low insertion loss, large operational bandwidth, small device footprint, and ease of fabrication. The two types of diodes, reciprocal and nonreciprocal optical diodes, have been proposed based on different mechanisms. The conventional nonreciprocal designs utilize magneto-optical effect [6–8] or nonlinearity [9–12]. The reciprocity of the Lorentz theorem is broken in such designs. More importantly, the optical isolator which prohibits the propagation of any possible mode in one direction can be achieved [13]. Meanwhile, the reciprocal optical diodes,

in which the time-reversal symmetry holds, have drawn increasing attention in recent years. The underlying mechanism is the mode conversion in linear structures with spatial asymmetry [14]. In such kind of the optical diode, the unidirectional transmission naturally exists for only certain modes. Due to the flexibility of designing coupling structures and tuning the photonic properties, the two-dimensional (2D) photonic crystal (PhC) has been shown as a promising building block to realize the optical diode. In this chapter, we will provide a summary of proposed schemes of both reciprocal and nonreciprocal optical diodes based on the 2D PhC slabs. This chapter is organized as follows: Section 2 will focus on the reciprocal optical diode based on the 2D PhC composed of dielectric rods or air-holed dielectric slab; Section 3 will introduce nonreciprocal optical diode based on nonlinear effects.

2. Reciprocal optical diode

Any reciprocal device based on passive and linear structure holds the time-reversal symmetry because the materials are described by scalar permittivity and permeability. The function of such reciprocal device has been proven and can be described by converting one set of orthogonal input modes to a matching set of orthogonal output modes [14]. In waveguide structure, the conversion between low-order even and odd modes is usually utilized. For an ideal reciprocal optical diode, complete conversion of a specific mode in one direction and meanwhile complete reflection of the same mode in opposite direction are required. An example of optical diode is illustrated in **Figure 1**. Modes A and B are used to denote the even mode and odd mode, respectively. The even mode A incident from the left port is converted into odd mode B on the right, while the odd mode B from the left is completely reflected. Meanwhile, the transmission of even mode A is not allowed from right to left, while the odd mode B from the right is converted to even mode A. It can be seen that the diode effect for even mode is achieved in this device. The symmetric even-to-odd mode and odd-to-even mode conversions reflect the time-reversal symmetry. It should be noted that this linear and passive device cannot block all possible modes in one direction, which means it is not an optical isolator. In this section, we will focus on the proposed schemes and designs in the last decades, which are based on the 2D PhC composed of dielectric rods or air-holed dielectric slab.

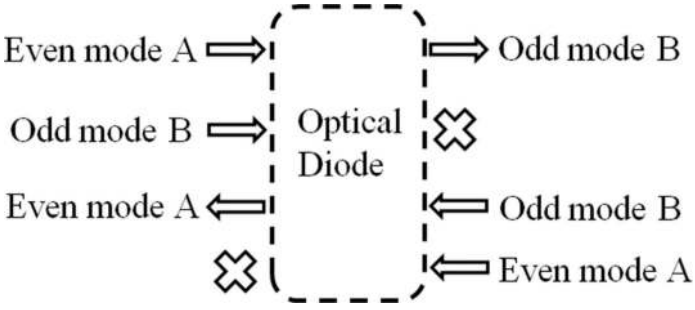

Figure 1. The functionality of a simple reciprocal optical diode of even mode.

2.1. Rod-type PhC optical diode

The rod-type 2D PhC represents the crystal consisting of periodic dielectric rods immersed in air. The rod material is commonly set as silicon in the below designs. The polarization of light is usually the chosen TM mode whose electric field is parallel to the rod. This is determined by the bandgap of such kind of PhC. The optical properties can be simulated by finite element method (FEM) or finite-difference time-domain (FDTD). Almost all simulations of rod-type designs discussed here are within two-dimensional. The length of rod is assumed infinite. Moreover, when estimating the performance of diode effect, two terms "unidirectionality" and "contrast ratio" may be used. The unit of unidirectionality is dB, and the expression is $U = 10\log_{10}(T_{for}/T_{back})$. The contrast ratio is defined as $CR = (T_{for} - T_{back})/(T_{for} + T_{back})$. The contrast ratio of an ideal optical diode is 1.

Feng and Wang [15] proposed a device with the abilities of wavelength filtering and unidirectional light propagation based on the 2D square-lattice PhC with a rectangular defect. In the L-type device shown in **Figure 2**, the left W1-typed waveguide formed by removing one row of rods only sustained an even-mode guiding band spanning the frequencies from 0.3020 c/a to 0.4160 c/a. The under waveguide constructed by removing one row of rods and shifting the adjacent two rows of rods outward for the distances of 0.7a and 0.35a could hold the odd-mode guiding bands from 0.3308 c/a to 0.4160 c/a and even-mode guiding bands within the frequencies from 0.2746 c/a to 0.4160 c/a. The rectangular defect was located at the corner to connect two waveguides. The two side lengths of the rectangle were 1.367a and

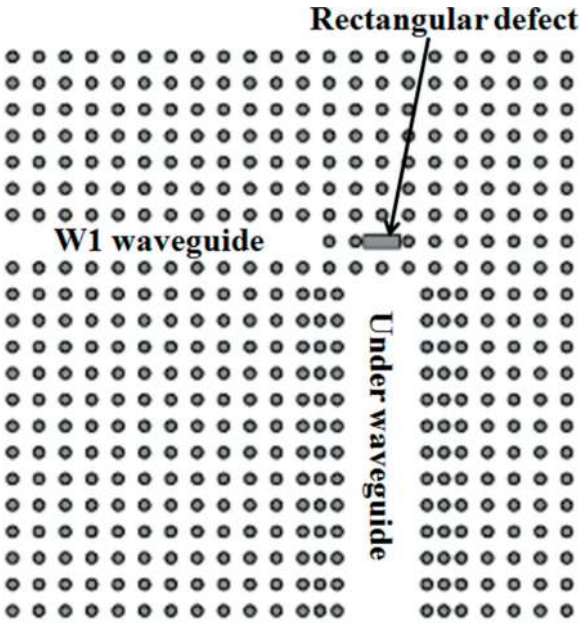

Figure 2. Coupling structure consists of PhC waveguides with the rectangular defects [15].

0.5a, respectively, and the long side was placed along the x-direction of the PhC. There were four defective modes localized by this defect. The adopted mode was located at 0.3977 c/a, and the symmetry was odd in the horizontal direction and even along the vertical direction. The unidirectional propagation of the fundamental mode (even mode) for TM polarization was realized at 0.3977 c/a. The insertion loss was about −6 dB in forward direction, and about 25 dB unidirectionality was achieved. Moreover, the resonant frequency can be linearly tuned by adjusting the coupling region between the defect and the input waveguide. Due to the coupling between defect/cavity and waveguide, the operational bandwidth is narrow.

Ye et al. [16] realized the optical diode effect for even mode by a 2D PhC structure comprising two line-defect waveguides (W1, W2) and a simple defect cavity, as shown in **Figure 3**. Here, the numbers of rows for removed rods were 1 and 2 in W1 waveguide and W2 waveguide, respectively, and the cavity was made by removing two central rods. From left to right, the structure was divided into five parts: W2 waveguide, four-column length matching stage, W1 waveguide, cavity, and W2 waveguide. The mode conversion was impelled by the similarity between the odd mode in the W2 waveguide and the second cavity mode with even symmetry in the horizontal direction and odd symmetry in the vertical direction at the resonant frequency 0.3930 c/a. When the even mode was inputted from the left port at this frequency, it would couple to the second mode in the cavity and then coupled to odd mode in the W2 waveguide. The unidirectional propagation of even mode was achieved thanks to the W1-cavity-W2 design breaking spatial symmetry. The full width at half maximum of the forward transmission spectra of the proposed design with incidence of even mode was about 0.0002 c/a. The transmission efficiency reached a peak 92.5% at the resonant frequency in forward direction, while the value stayed below 0.1% within the frequency range from 0.3900 c/a to 0.3960 c/a for the backward transmission, and the unidirectionality reached approximately 35 dB at resonant frequency. The resonant frequency could be tuned by changing the radii of the nearest rods surrounding the defect and shape of the cavity according to the equation

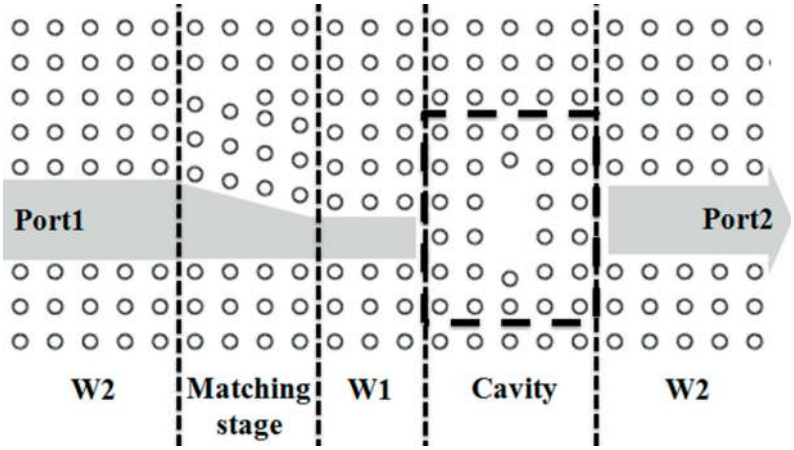

Figure 3. Coupling structure consists of PhC waveguides with the cavity [16].

$$f = 0.3889 + 0.464(r/a) - 2.2167(r/a)^2 (0.18a < r < 0.22a)$$
$$f = 0.4112 - 0.0999(\Lambda/a) + 0.0459(\Lambda/a)^2 (0.1a < \Lambda < 0.3a), \quad (1)$$

where r denoted the radius of the nearest rods surrounding the defect and Λ was the movement of two neighboring rods. The maximum forward transmission efficiencies of all of the tuned structures exceeded 90%. Due to the narrow bandwidth, the proposed design could be used for mode converter, optical diode, and waveguide filter.

Khavasi et al. [17] reported a broadband optical diode based on pure PhC waveguide with spatial asymmetry as illustrated in **Figure 4**. The components of the design mainly included a mode converter, a mode filter, a four-column length matching stage, and line-defect waveguides formed by removing two rows (W2) and one row (W1) of rods. Along the forward direction, the PhC structure could be divided into seven parts: W2, matching stage, W1, mode converter, W2, mode filter, and W2. The two different routes, U-shaped and straight paths, introduced the phase shifting in the mode converter with 5×5 unit cells. The geometrical lengths of the left, upper, and right arms of the U-shaped path were 3a, 2a, and 2a, respectively. And, two $\pi a/2$ components were added to account for the two quarter-circle paths to be traveled at each bend. The length of the straight path was around 4a. The required phase difference for mode conversion was induced by the different length according to the equation $\Delta\phi = \beta_1 \cdot \Delta L \approx 3\pi$, where $\beta_1 = 1.535/a$ was the propagation constant of the waveguide at the normalized frequency $\omega_n = a/\lambda = 0.367$. The mode filter was designed by placing a row of rods with $r = 0.18a$ in the middle of W2. The electric field profile of the odd mode was zero at the middle of the waveguide, while the

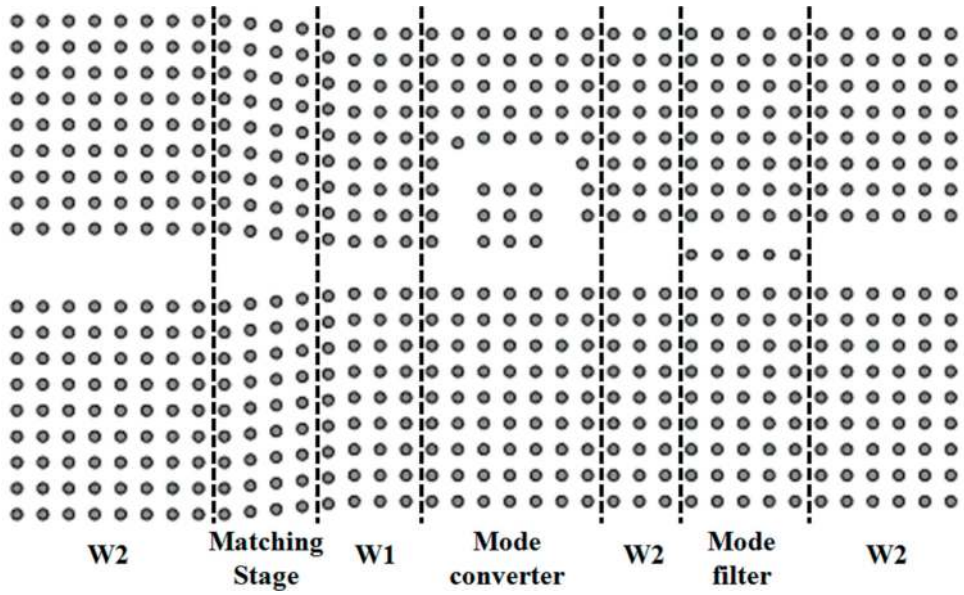

Figure 4. The broadband optical diode with U-shaped and straight split paths [17].

electric field profile of the even mode reached its maximum and was reflected back. Thus, the even mode excited at the left port converted into odd mode by the mode converter and pass through the mode filter, while the even mode was reflected back by the mode filter in the opposite direction, which achieved the optical diode effect. The transmission efficiency kept higher than 94% in the range of frequency $0.366 < \omega_n < 0.381$, and the achieved level of unidirectionality was approximately 78 dB.

Lu et al. [18] realized the optical diode effect based on two-dimensional square-lattice PhC, in which a directional coupler and 90° bend were utilized to realize the mode converter and mode filter functions. The scheme is depicted in **Figure 5**. The components in leftward direction were, respectively, W2 waveguide formed by removing two rows of rods, mode filter and mode converter, and W1 waveguide created by removing one row of rods, a four-column length adiabatic-matched region and W2. A perpendicular W1 waveguide and two 90° bends were combined together to achieve a mode converter. The conversion principle was as follows: when the light transmitted in the leftward direction, the odd mode was even symmetric along the horizontal direction in the mode filter, while the fundamental even mode in the perpendicular W1 waveguide was also symmetric about the parallel direction. Therefore, the odd mode could be thoroughly converted into the even mode after the 90° waveguide bend. On the other hand, the even mode would be converted into odd mode based on the same theory in the rightward direction. The mode filter was designed by placing a row of rods in the middle of W2 as several other works. For the device, the odd mode was completely transmitted in forward direction (left to right) and converted to the fundamental even mode but was blocked in the opposite direction. Approximate 95% forward transmission efficiency, 0.024 c/a operational bandwidth, and maximum 80 dB unidirectional extinction ratio were achieved in 2D simulations.

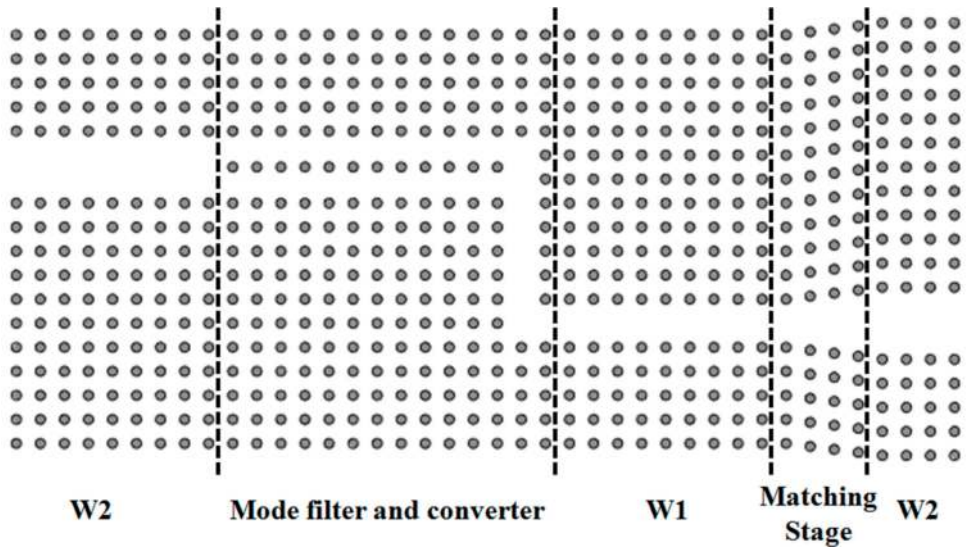

Figure 5. The broadband optical diode with a directional coupler and double 90° bends [18].

Kurt et al. [19] reported a photonic structure formed by using a chirped PhC waveguide to realize asymmetric light propagation as shown in **Figure 6**. A distance increment between each neighboring column of the dielectric rods, which caused that the waveguide mode moved toward the outside of the bandgap, was introduced to break the spatial symmetry. Here, the distance between each unit cell was still a constant along the y-direction ($\Delta y = a$), while the interval of rods linearly increased along the x-direction ($0.5a < \Delta x < 2.5a$), and the total length of the chirped PhC waveguide was approximately 16a. Thus, the structure became sparse along the x-direction, and the spatial distribution was uniform along the y-direction. When the light traveled in forward direction, the light mainly propagated at the center and leaked toward the two sides of the waveguide after propagating a section of distance; then, it traveled again along the x-direction and reached the end of the structure. The amount of light reaching the waveguide centerline was very small. However, the central lobe strongly appeared at the waveguide exit in the backward light transmission. The contrast ratio was around 0.75 at the operating frequency $a/\lambda = 0.3288$.

Giden et al. [20] from the same research team as the above work theoretically and experimentally realized the asymmetric light transmission based on PhC with a gradient index distribution along the x-direction, in which the waveguide was formed by introducing point and line defects. The total length and width of the proposed structure were L = 16a and W = 20a, respectively. Continuously graded refractive index distribution could be approximated by relocating the PhC dielectric rods. In order to achieve a desired index profile within certain wavelength, they utilized an equation $n(x) = n_0 \,\mathrm{sech}(\alpha x)$, to formulate the hyperbolic secant index profile and then to modulate the spatial distributions of PhC cells, where the constant $\alpha = 0.0373a^{-1}$ was the gradient factor and n_0 was the effective refractive index at x = 0. The effective refractive indices at $x = 0$ and 16a were set as $n(x = 0) = n_0 = 2.20$ and $n(x = L = 16a) = 1.41$. The distance between each rod along x-direction was modified to find the targeted longitudinal index distribution, and the lateral interval was fixed at a. After the spatial distributions of the silicon rods were determined, a line defect was introduced by removing one row of rods to

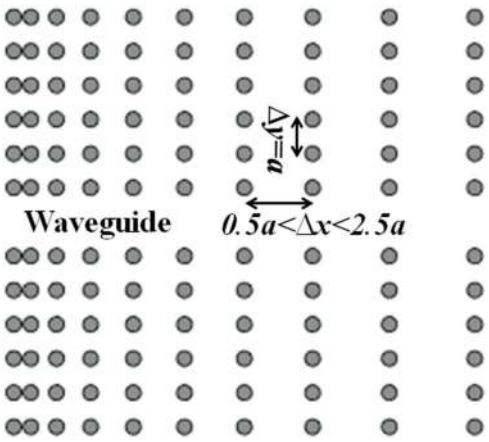

Figure 6. The optical diode in PhC waveguide with chirped PhC structure [19].

form a waveguide. The asymmetric propagation was achieved due to the broken spatial symmetry and the forward (left-to-right) and backward (right-to-left) transmission efficiencies reached 7.26% and 24.8% at the peak, respectively. The contrast ratio was in the range of 0.412–0.773 within the telecom wavelength range from 1523.5 nm to 1576.1 nm in simulation. Moreover, the point defects were inserted by shifting the positions of adjacent rods along the y-direction to increase the difference between forward and backward transmissions. In experiment validation (microwave regime), the proposed design had 4.11% and 49.8% forward and backward transmission efficiencies, respectively, exceeding 0.80 contrast ratio within the operating frequency band from 12.8 to 13.3 GHz.

Soltani et al. [21] proposed a 2D PhC made of elliptic silicon rods to realize the unidirectional propagation as depicted in **Figure 7**. The major and minor axes of the ellipse were 0.31a and 0.22a, respectively. The waveguide was created by removing one row of the dielectric rods along the x-direction. The distance between neighboring columns was modulated according to the equation, $d = 0.6a + (n-1) \times 0.2a$, where n represented the nth interval in the x-direction and over all the structure $0.6a \le d \le 2.2a$. Meanwhile, a reflector between two successive columns was introduced to control losses of the scattered light. Thus, the asymmetric spatial distribution of the unit cells ensured the one-way light transmission. When the light was inputted from the left port, it propagated along the centerline of the structure, and then the flow of light leaked into the larger space between rods after several periods. Thus, the light was blocked in this direction. In the opposite direction, the light source was positioned on the right side of the structure; the light emitted was widely spread in the beginning until it reached the center of the structure. The transmission efficiency was lower than 10% in forward direction (left to right), while the value reached 80% in the opposite propagation within the frequency region from 0.28a/λ to 0.32a/λ. Finally, they studied the effects of the orientation of ellipses on the transmission of light and found that the orientation angle may introduce shift and oscillation to the transmission spectra.

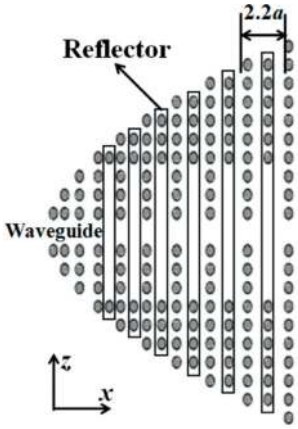

Figure 7. The optical diode in PhC waveguide with elliptic rods [21].

Singh et al. [22] realized the optical diode effect based on a hexagonal and square-lattice PhC structures with silicon rods immersed in air. The structure is demonstrated in **Figure 8**. The waveguide was formed by removing one row of rods and chirping the neighboring rods, which was realized by changing the radii of the rods. Two kinds of devices were proposed according to the different lattice. For the regular hexagonal lattice PhC, the lattice constant a and radius of the rods r were 0.68 μm and 0.23 μm, respectively, and the radii of the chirped rods were $r_1 = 0.220$ μm, $r_2 = 0.209$ μm, and $r_3 = 0.197$ μm. When light propagated from left to right (forward direction), it mainly propagated along the central region of PhC waveguide, and a high power was obtained from output port. In the opposite direction, the light leaked in the designed structure so that the field amplitude along the propagation direction was weak. Approximate 82% forward transmission efficiency and lowest value 35% in the backward direction were obtained at 1.55 μm. The relative extinction ratio was nearly 5.5 dB. For the square arrangement-based optical diode, the lattice constant a and radius of the rods r were 0.71 μm and 0.22 μm, respectively, and the radii of the chirped rods were $r_1 = 0.21$ μm, $r_2 = 0.20$ μm, $r_3 = 0.19$ μm, and $r_4 = 0.17$ μm. Here, around 52% forward transmission efficiency and 4.1 dB extinction ratio were achieved at 1.55 μm. Then, they showed that the engineering of chirping parameters not only in terms of rods' radii, but also other parameters such as lattice spacing and refractive index parameters may give rise to the superior performance of the optical diode-like photonic structures.

Liu et al. [23] devised an ultracompact mode converter based on a two-dimensional square-lattice PhC made of dielectric rods in air by a two-phase numerical optimization method and applied it to the optical diode. In numerical design and optimization, the design was evaluated by the error metric, $J = \sum_{\omega} (1 - P_{\omega})^2$, where P_{ω} was the conversion efficiency at frequency ω. A region with rods located on the 20 possible lattice sites was considered to limit the design space in the optimization process. In the first phase, a combinatorial search is performed using simulation method to analyze every possible combination of rods (presence or absence) on the 20 lattice sites in the region. Any structures with desirable conversion behavior ($J \leq 0.5$) were considered potential candidates for further optimization. In the second phase, a further optimization adjusted the radii of the existing rods in the initial combinatorial to minimize the error metric J. They obtained a compact mode converter with above 99% conversion efficiency, which occupied an area of 4×10 unit cells' large functional region (spatial inverse symmetry was hold). For optical diode design, they adopted the same optimization strategy, and the

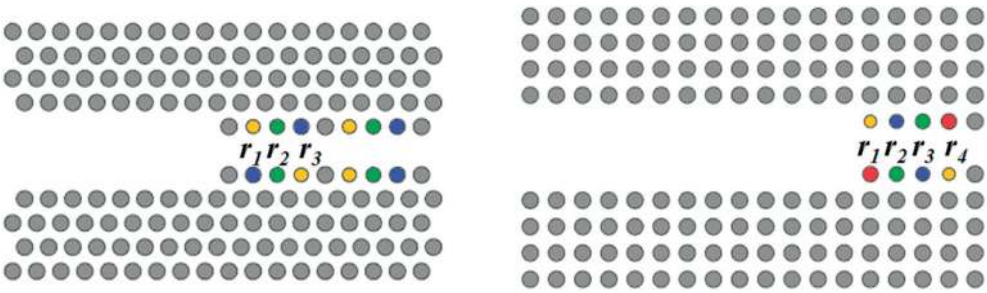

Figure 8. The optical diode in PhC waveguide with chirped rods with different symmetries [22].

more than ten structures with ideal performance were found, which occupied 4 × 5 unit cells' large functional region as demonstrated in **Figure 9**. The forward mode conversion efficiency exceeded 97%, and backward reflection was about 3% at frequency 0.4025 c/a. The operational bandwidth was larger than 0.015 c/a.

Ye et al. [24] demonstrated a compact broadband optical diode based on linear 2D rod-type PhC as shown in **Figure 10**. The proposed structure consisted of a simple waveguide made by removing two rows of rods and a 4 × 1 unit cells' large functional region, the spatial dielectric distribution in which was numerically optimized by finite element method (FEM) combining

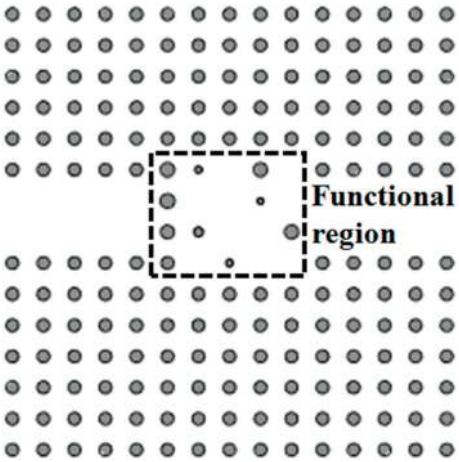

Figure 9. The broadband optical diode in PhC waveguide with 4 × 5 unit cells' compact-optimized functional region [23].

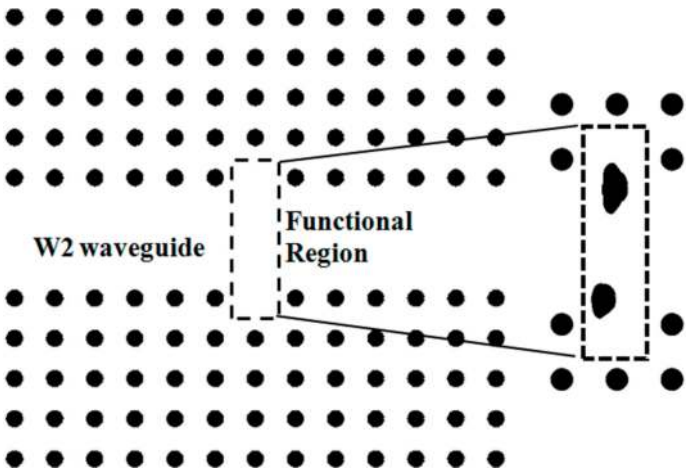

Figure 10. The broadband optical diode in PhC waveguide with 4 × 1 unit cells' compact-optimized functional region [26].

the geometry projection method (GPM) [25] and the method of moving asymptotes (MMA) [26]. Two dielectric rods inside the functional region were still kept during the optimization process. The GPM employed 6 × 20 control points whose heights can be fitted as a three-dimensional surface and the intersection line of level plane and three-dimensional surface could be used to define the rod shape. When level plane was set at zero, the dielectric constant at coordinate x could be formulated as $\varepsilon(x) = \varepsilon_{air} + \frac{(\varepsilon_{si}-\varepsilon_{air})}{2}\left(\tanh\left[\frac{sign[S(x)]d(x)}{\xi}\right]+1\right)$, where S(x) was the surface function, d(x) was the minimum distance from the refined surface to the nearest intersection curve, and ξ was the control parameter of vanishing of intermediate dielectric at interface. The GPM controlled the rod shape, size, and position by adjusting the heights of the control points. The FEM and MMA were utilized to determine the heights of control points to find the solution. The optimization process proceeded in two phases to obtain large operating bandwidth. First, they searched a candidate at the center frequency 0.40 c/a; in the second phase, they optimized further by the new objective function, which was the weighted average of objective function values at five frequencies within the targeted frequency domain. The integrals of power flux for desired optical behavior were set as objective functions during the optimization process. The maximum forward transmission efficiency was 83%, and the above 60% transmission efficiency within bandwidth 0.01 c/a was achieved. The above 19 dB unidirectionality (maximum 30 dB) for even mode was achieved within bandwidth 0.01 c/a as well.

Wang et al. [27] demonstrated a graded photonic crystal (GPhC) design with 11a × 25a large scale, which was obtained from a conventional square-lattice PhC with $R = 0.2a$ by linearly changing the radius of dielectric rods, to achieve unidirectional light propagation. The structure is demonstrated in **Figure 11**. The radii of the dielectric cylinders in the x-y plane were given by$R_{(x+1)a} - R_{xa} = 0.01a$ (in x-direction, $R_{1a} = 0.2a$) and $R_{(y+1)a} - R_{ya} = 0.01a$ (in +y-direction),

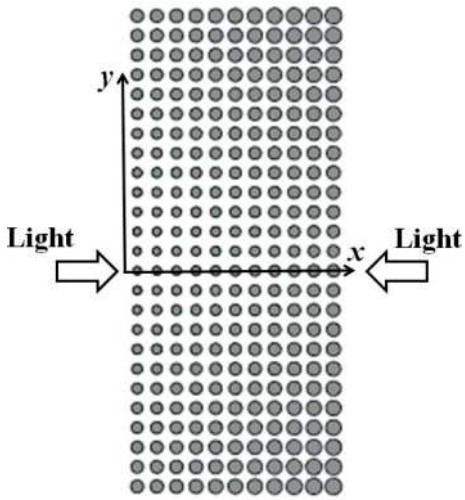

Figure 11. Asymmetric light propagation based on graded PhC [27].

where R_{xa} was the radius of dielectric rods of xth period. The structure in +y-direction was symmetrical along the x-axis with the structure in the −y-direction. Here, the x-axis was located at the middle of the structure along the y-direction. The transverse field profiles demonstrated a significant difference. When the light propagated from left to right (forward direction), most of the light at the x-axis propagated across the structure, and the light on the two sides of the x-axis could not propagate after several periods because of the directional bandgap. The light almost converged into the middle position at the end face of the structure. On the other hand, when the light propagated in backward direction (right to left), only the light along the optical axis transmitted into the GPhC structure, and the light propagating into GPhC spread to both ends of the structure after a few periods, the light could be scarcely detected at the end face. The intensity at the convergence spot of the light propagated in forward direction was almost 14 times more than the maximum intensity of the backward transmission light. Maximum 0.7 contrast ratio was achieved at the frequency of 0.395 (a/λ). If the numbers of period were extended to 13 in the horizontal direction, higher contrast ratio (near 1) was attained at the frequency of 0.394 (a/λ).

2.2. Air-holed PhC optical diode

Most of the designs based on rod-type PhC discussed above were confined in simulation because of the difficulties in fabricating. The only experimental validation was reported in Giden's work [20], but operating in the microwave regime (10 GHz). Moreover, the absence of light confinement along the rod direction is another limitation. Compared with rod-type PhC, the fabrication technique of air-holed PhC slab is more mature and compatible with conventional CMOS processing. Air-holed PhC is formed by etching periodic air holes in dielectric slab. The optical diode based on air-holed PhC can be directly connected to standard silicon waveguide, showing its ability of integration with other silicon-based photonic devices. However, unfortunately, lack schemes for air-holed 2D PhC optical diode can be found. One scheme is based on the PhC heterostructure with directional bandgap [28–31], and the other scheme is based on topology optimization [32]. The TE mode whose magnetic field is perpendicular to the slab is considered in all designs discussed in this section and most simulations are performed in 3D FDTD.

Cicek et al. [31] realized the unidirectional light transmission in a 2D PhC heterostructure with air holes in an AlGaAs host. The proposed structure was constructed of two kinds of photonic crystals (PhC1, PhC2) with the same orientation and lattice constant but different radii of air holes, as illustrated in **Figure 12**. The interface was located along its body diagonals. The radius of air holes in PhC1 with 16 × 16 unit cells was set as 0.460a, while the value in PhC2 with 15 × 15 unit cells was 0.352a. Moreover, PhC2 was offset by $d = 0.2a$ to decrease the forward reflection losses introduced by effective index variation. In order to achieve the asymmetric light propagation, stop band for blocking light transmission in backward direction (right to left) was studied. When the light propagated in forward direction (left to right), it transmitted toward the PhC2 and eventually the output port. The waves were self-collimated in both PhC1 and PhC2 at the frequency $0.37\omega a/2\pi c$. While, in the opposite direction, the incident light was reflected at the air-PhC2 interface, the deflected wave components at the air-PhC2 interface could reach PhC1 and eventually the output port. However, several lights

would leak out in the reverse direction. The transmission efficiency in forward direction was around 50% within the frequency region from 0.32ωa/2πc to 0.42ωa/2πc, while the value in backward direction kept lower than 20%. The maximum of contrast ratio was achieved approximately 0.90. Lu et al. [28] experimentally fabricated similar structure using poly[2-methoxy-5-(2-ethylhexyloxy)-1,4-phenylenevinylene] MEH-PPV PhC. In the experiment, the lattice constant was 440 nm, and the radii of air holes for PhC1 and PhC2 were 110 nm and 170 nm, respectively. The angle between the hetero-interface and the horizontal direction was 56°. The transmissions of 50% and 0.02% were achieved for the rightward and leftward incidence within the wavelength region from 640 nm to 660 nm.

Wang et al. [29, 30] proposed an optical diode design with functional region $6 \times 6\ \mu m^2$ based on silicon PhC slab. The radii of air hole for PhC1 and PhC2 were 0.24*a* and 0.36*a*, respectively. The hetero-interface was placed between PhC1 and PhC2 along the Γ-M direction. Two 4*a*-wide waveguides were located at the two sides of the structure and were used to enter or exit the light beam. There exists an isolation band ranging from 0.2649 to 0.2958 (a/λ), where the transmission efficiency in forward direction (left to right) reached a peak about 6%, while the backward transmission kept between 0.5% and 1% within the frequency region from $0.2649a/\lambda$ to $0.2958a/\lambda$. The maximum contrast ratio 0.846 was obtained at the peak. Then, the original diode was optimized in order to decrease the backward transmission to be zero and increase the peak of forward transmission as much as possible. The revised structure is demonstrated in **Figure 13**. The backward transmission generally decreased a half compared with that of the original structure, and the forward peak reached approximately 13%. The maximum contrast ratio of the revised structure increased to 0.92 at the peak. In the experiment, the patterns were

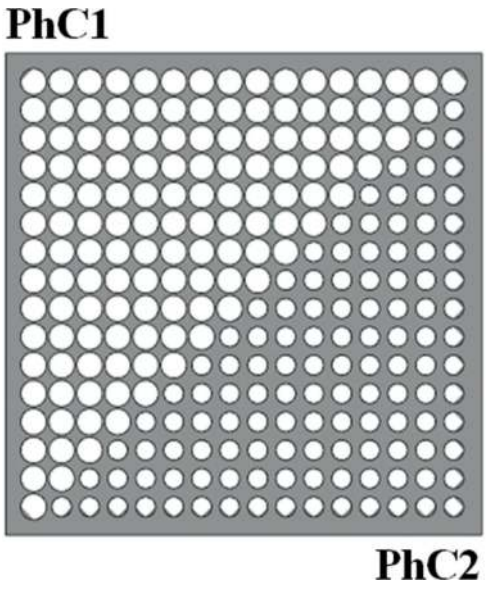

Figure 12. Refraction-based optical diode with PhC heterostructure [31].

defined in resist using the electron beam lithography (EBL) on the silicon-on-insulator (SOI) chip and then transferred to silicon layer using the inductively coupled plasma (ICP) reactive ion etching. To form an air-bridged structure, the SiO_2 underneath the patterned PhC was finally removed. The maximum forward transmission efficiency in experiment with asymmetric input/output waveguides approached 21.3%, and the best contrast ratio of the diode structure reached 0.885 at the peak.

Ye et al. [32] realized the optical diode effect in 2D silicon PhC slab waveguide with 1.2a × 2.8a large functional region, in which there was only one deformed air hole. The structure is illustrated in **Figure 14**. The waveguide was constructed by removing one row of air holes along x-direction and moving the first and second nearest row with 0.15a and 0.1a in y-direction, respectively. The spatial dielectric distribution in the functional region was numerically optimized by finite element method (FEM) combining the geometry projection method (GPM) and the method of moving asymptotes (MMA). The GPM employed 13 × 29 control points to fit the three-dimensional surface. The optimization algorithm MMA was utilized to determine the heights of all control points in GPM. In order to find a broadband optical diode, three optimization steps were taken: first, they searched a bidirectional mode converter with mirror symmetry in functional region at the center frequency 0.36 c/a. Next, the symmetry was broken to find the solution for optical diode working at center frequency. The last step was to extend the operational frequency range from single frequency. Here, the integrals of power flux for desired optical behavior were set as objective functions. The above 89.9% forward transmission efficiency, 0.01 c/a operational bandwidth, and maximum 24 dB unidirectionality were achieved in 2D FEM simulations. In the air-bridged 3D FDTD model, the maximum unidirectionality was about 19.6 dB, while the value kept higher than 12.7 dB for slab thickness 0.54a. It should be noted that identical performance of 3D device and 2D optimized structure remains a challenge.

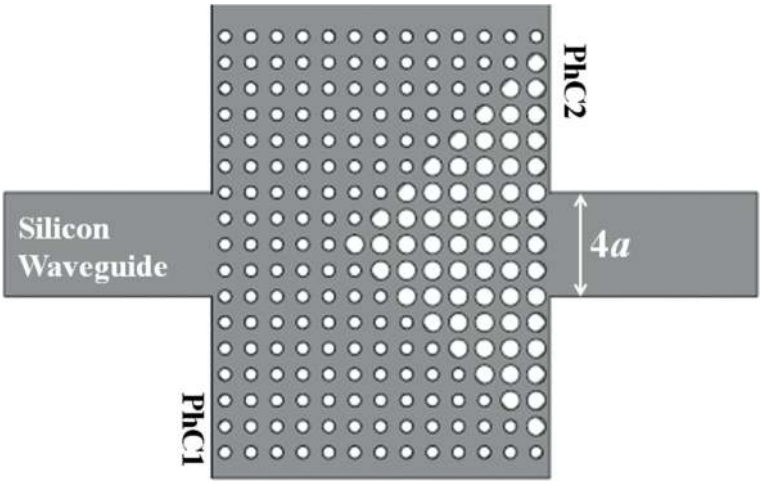

Figure 13. Optical diode with PhC heterostructure connecting standard silicon waveguide [29].

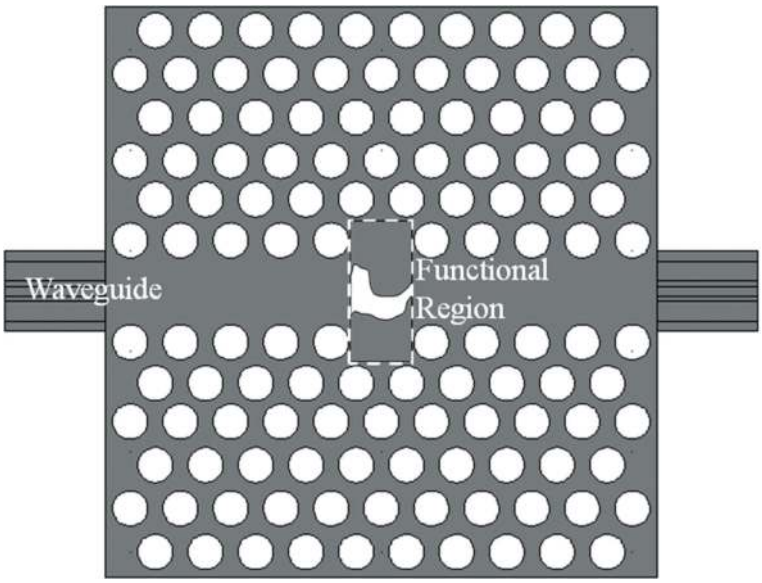

Figure 14. Optical diode with topological optimized functional region connecting silicon waveguide [32].

3. Nonreciprocal optical diode

The optical diode effect achieved in linear and passive PhC (discussed in Section 2) cannot break the reciprocity of the Lorentz theorem and consequently cannot play as an important optical device: the optical isolator. The conventional nonreciprocal designs utilize magneto-optical effect or nonlinearity. Unfortunately, common waveguide materials, especially Si, SiO_2, and Si_3N_4, present only relatively weak or even no magneto-optical effect. Meanwhile, the prerequisite external magnetic field would limit the integration for on-chip applications. Therefore, we will focus on the nonlinearity in this section. The major effects may include the second-order optical nonlinearity, the Kerr effect, two-photon absorption, free-carrier effect, and thermo-optic effect [33]. These effects have been pervasively employed in on-chip all-optical processing such as wavelength conversion, optical switch, modulation, and optical isolation [34–36].

Zhang et al. [37] proposed a silicon optical diode based on optical nonlinearity in cascaded PhC L3 cavities, which was formed by removing a line of three holes as demonstrated in **Figure 15**. The lattice constant was 420 nm, and the air-holed radius was 126 nm. The three air holes adjacent to the right cavity were shifted by 0.175*a*, 0.025*a*, and 0.175*a*, respectively. And, the footprint of the whole device was about 20 μm × 10 μm. The resonant wavelengths of two cascaded L3 cavities did not match exactly due to the different distribution of the holes in periphery. When the input power was low, the two L3 cavities were both working in the linear regime, and asymmetric transmission was not realized. As input power increased, the resonance dips redshifted due to the onset of nonlinearity induced by the thermo-optic effect in the silicon cavities. A nonreciprocal transmission ratio (NTR) of 30.8 dB and insertion loss of 8.3 dB was

realized in the device. The device had a relatively broad 17 dB operation bandwidth of 0.08 nm, and at least 16 dB of NTR was achieved when input power varied between −6.25 and −2.95 dBm.

Bulgakov and Sadreev [38] proposed an all-optical diode in asymmetric L-shaped PhC waveguide with a single nonlinear Kerr microcavity at the corner. The structure is depicted in **Figure 16**. The linear L-shaped PhC waveguide was formed by removing one row of dielectric rods, and the microcavity was constructed by three linear rods and one nonlinear rod. The radius and dielectric constant of the GaAs rods were 0.18a and 11.56 in the PhC, where the lattice unit was set as 0.5 μm. The nonlinear defect rod had the radius 0.4a, and the dielectric constant was 6.5. The nonlinear refractive index was 2×10^{-12} cm^2/W. In order to achieve the asymmetric design of the microcavity, the dielectric constant of the third additional rod inside the right leg of the waveguide was chosen as 5. The two dipole eigenfrequencies of the microcavity were $0.3658 \times 2\pi c/a$ and $0.3650 \times 2\pi c/a$, respectively. When both dipole modes were excited simultaneously, the design could be opened for light transmission at some magnitudes of frequency and injected intensity because of the nonlinear coupling between them. The opening region mostly depended on the ratio between the nonlinearity constant and the coupling strengths of the dipole modes with the propagating waveguide modes. Therefore, the asymmetric transmission in the design was achieved due to the different threshold for light transmissions from left to right and backward. This came from different coupling strengths of dipole modes with the propagating mode of the left and right waveguide legs. In the design, the direction of optical diode transmission could be controlled by power or frequency of injected light.

Liu et al. [39] realized the optical diode effect based on asymmetrical coupling by a microcavity with nonlinear Kerr medium and a FP cavity at two sides of PhC waveguide. In the system, a Fano resonant microcavity with ultrahigh-quality factor was designed in rod-type PhC. An elliptical point defect was placed in the first layer below a line-defect PhC waveguide, and a FP

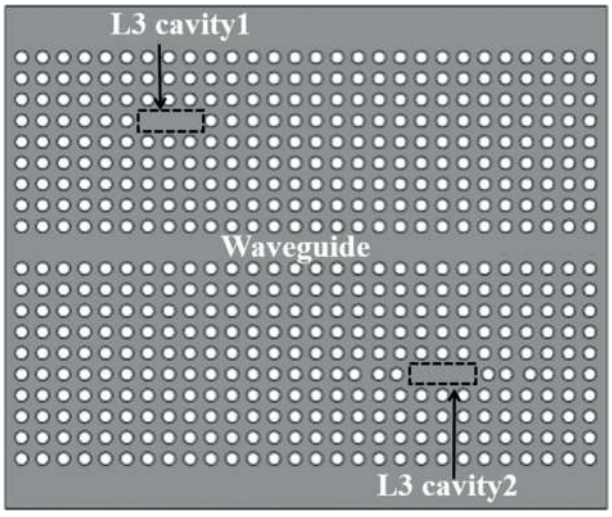

Figure 15. Silicon optical diode based on cascaded photonic crystal cavities [37].

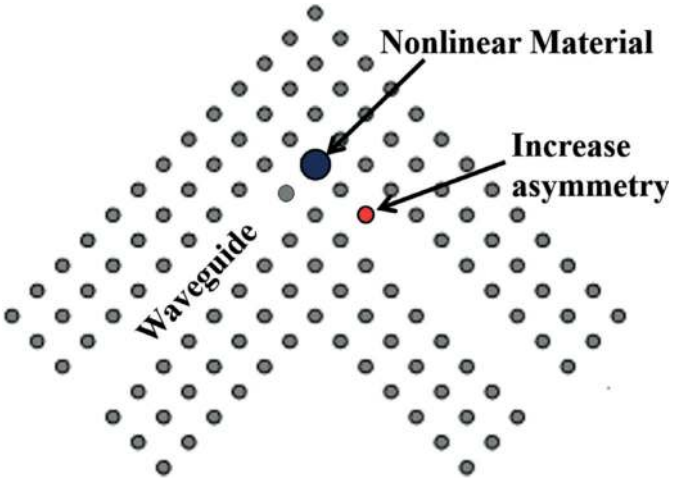

Figure 16. Optical diode based on dipole modes of Kerr microcavity in asymmetric L-shaped PhC waveguide [38].

cavity was located in the second layer above PhC waveguide, as shown in **Figure 17**. Moreover, a reflector layer was set below the left end of FP cavity to form asymmetric structure. The radius of dielectric cylinder was 0.3a; the major and minor axes of elliptical point defect were set as 0.534a and 0.3a, respectively. Because of the asymmetric design, backward (right to left) propagation required stronger incidence light to excite Kerr effect of microcavity than forward (left to right) transmission, so the unidirectional transmission could be realized. The high transmission in forward direction was approximately about 80%, and maximum contrast ratio was about 0.8.

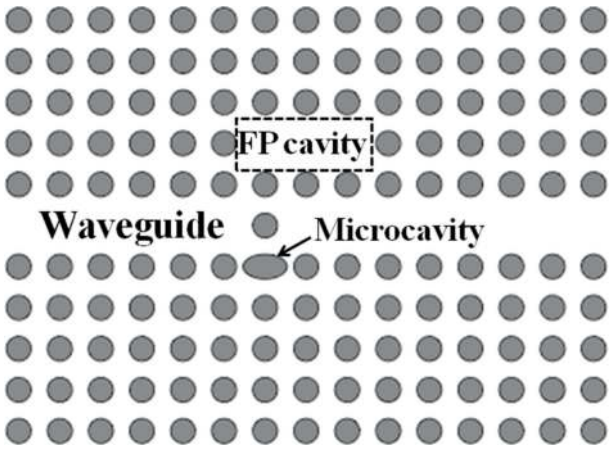

Figure 17. Optical diode based on asymmetrical coupling by a microcavity and FP cavity at two sides of PhC waveguide [39].

4. Conclusion

In this chapter, the proposed schemes for optical diodes based on 2D PhC have been briefly summarized. For reciprocal optical diode, we introduce 11 designs based on rod-type PhC and 4 designs based on air-holed PhC slab. Since the linear and passive structures hold the time-reversal symmetry, the unidirectional transmission of certain optical mode is achieved by spatial asymmetric mode conversion. For nonreciprocal optical diode, we mainly focus on the PhC cavity with optical nonlinear effects. The three designs can be used as optical isolator since it can block all possible modes in one direction. Considering the performances, new schemes for 2D PhC optical diodes with high contrast ratio, low insertion loss, large operational bandwidth, small device footprint, and ease of fabrication are still highly desirable.

Author details

Han Ye*, Yumin Liu and Zhongyuan Yu

*Address all correspondence to: han_ye@bupt.edu.cn

State Key Laboratory of Information Photonics and Optical Communications, Beijing University of Posts and Telecommunications, Beijing, PR China

References

[1] Fedotov VA, Mladyonov PL, Prosvirnin SL, Rogacheva AV, Chen Y, Zheludev NI. Asymmetric propagation of electromagnetic waves through a planar chiral structure. Physical Review Letters. 2006;**97**(16):167401

[2] Hwang J, Song MH, Park B, Nishimura S, Toyooka T, Wu JW, et al. Electro-tunable optical diode based on photonic bandgap liquid-crystal heterojunctions. Nature Materials. 2005;**4**(5):383-387

[3] Bi L, Hu JJ, Jiang P, Kim DH, Dionne GF, Kimerling LC, et al. On-chip optical isolation in monolithically integrated non-reciprocal optical resonators. Nature Photonics. 2011;**5**(12):758-762

[4] Xu J, Zhuang X, Guo P, Huang W, Hu W, Zhang Q, et al. Asymmetric light propagation in composition-graded semiconductor nanowires. Scientific Reports. 2012;**2**:820

[5] Fan L, Wang J, Varghese LT, Shen H, Niu B, Xuan Y, et al. An all-silicon passive optical diode. Science. 2012;**335**:447-450

[6] Haldane FDM, Raghu S. Possible realization of directional optical waveguides in photonic crystals with broken time-reversal symmetry. Physical Review Letters. 2008;**100**(1):013904

[7] Yu Z, Veronis G, Wang Z, Fan S. One-way electromagnetic waveguide formed at the interface between a plasmonic metal under a static magnetic field and a photonic crystal. Physical Review Letters. 2008;**100**(2):023902

[8] Wang Z, Chong Y, Joannopoulos JD, Soljacić M. Observation of unidirectional backscattering-immune topological electromagnetic states. Nature. 2009;**461**:772-775

[9] Lin XS, Wu WQ, Zhou H, Zhou KF, Lan S. Enhancement of unidirectional transmission through the coupling of nonlinear photonic crystal defects. Optics Express. 2006;**14**(6):2429-2439

[10] Wang J, Fan L, Varghese LT, Shen H, Niu B, Qi MH. A theoretical model for an optical diode built with nonlinear silicon microrings. Journal of Lightwave Technology. 2013;**31**:313-321

[11] Soljacic M, Luo C, Joannopoulos JD, Fan S. Nonlinear photonic crystal microdevices for optical integration. Optics Letters. 2003;**28**(8):637-639

[12] Sahoo PK, Joseph J. Optical diode using nonlinear polystyrene ring resonators in two-dimensional photonic crystal structure. Applied Optics. 2013;**52**:8252-8257

[13] Jalas D, Petrov A, Eich M, Freude W, Fan SH, Yu ZF, et al. What is—and what is not—an optical isolator. Nature Photonics. 2013;**7**(8):579-582

[14] Miller DAB. All linear optical devices are mode converters. Optics Express. 2012;**20**:23985-23993

[15] Feng S, Wang Y. Unidirectional reciprocal wavelength filters based on the square-lattice photonic crystal structures with the rectangular defects. Optics Express. 2013;**21**:220-228

[16] Ye H, Zhang JQN, Yu ZY, Wang DL, Chen ZH. Realizing mode conversion and optical diode effect by coupling photonic crystal waveguides with cavity. Chinese Physics B. 2015;**24**:094214

[17] Khavasi A, Rezaei M, Fard AP, Mehrany K. A heuristic approach to the realization of the wide-band optical diode effect in photonic crystal waveguides. Journal of Optics. 2013;**15**:075501

[18] Lu J, Ren HL, Guo SQ, Gu DY, Wen H, Qin YL. Ultra-wideband optical diode based on photonic crystal 90° bend and directional coupler. Chinese Optics Letters. 2014;**12**:102301

[19] Kurt H, Yilmaz D, Akosman AE, Ozbay E. Asymmetric light propagation in chirped photonic crystal waveguides. Optics Express. 2012;**20**(18):20635-20646

[20] Giden IH, Yilmaz D, Turduev M, Kurt H, Çolak E, Ozbay E. Theoretical and experimental investigations of asymmetric light transport in graded index photonic crystal waveguides. Applied Physics Letters. 2014;**104**:031116

[21] Soltania A, Ouerghia F, AbdelMaleka F, Haxhab S, Ademgilc H, Akowuahd EK. Effect of the elliptic rods orientations on the asymmetric light transmission in photonic crystals. Optics Communications. 2017;**392**:147-152

[22] Singh BR, Rawal S, Sinha RK. Chirped photonic crystal with different symmetries for asymmetric light propagation. Applied Physics A: Materials Science & Processing. 2016;**122**:605

[23] Liu V, Miller DAB, Fan S. Ultra-compact photonic crystal waveguide spatial mode converter and its connection to the optical diode effect. Optics Express. 2012;**20**:28388-28397

[24] Ye H, Wang D, Yu Z, Zhang J, Chen Z. Ultra-compact broadband mode converter and optical diode based on linear rod-type photonic crystal waveguide. Optics Express. 2015;**23**:9673-9680

[25] Frei WR, Johnson HT, Choquette KD. Optimization of a single defect photonic crystal laser cavity. Journal of Applied Physics. 2008;**103**:033102

[26] Svanberg K. The method of moving asymptotes-a new method for structural optimization. International Journal for Numerical Methods in Engineering. 1987;**24**(2):359-373

[27] Wang LH, Yang XL, Meng XF, Wang YR, Chen SX, Huang Z, et al. Asymmetric light propagation based on graded photonic crystals. Japanese Journal of Applied Physics. 2013;**52**:122601

[28] Lu CC, Hu XY, Zhang YB, Li ZQ, Xu XA, Yang H. Ultralow power all-optical diode in photonic crystal heterostructures with broken spatial inversion symmetry. Applied Physics Letters. 2011;**99**(5):051107

[29] Wang C, Zhou CZ, Li ZY. On-chip optical diode based on silicon photonic crystal heterojunctions. Optics Express. 2011;**19**(27):26948-26955

[30] Wang C, Zhou CZ, Li ZY. Linear and passive silicon optical isolator. Scientific Reports. 2012;**2**:674

[31] Cicek A, Yucel MB, Kaya OA, Ulug B. Refraction-based photonic crystal diode. Optics Letters. 2012;**37**(14):2937-2939

[32] Ye H, Yu Z, Liu Y, Chen Z. Realization of compact broadband optical diode in linear air-hole photonic crystal waveguide. Optics Express. 2016;**24**(21):24592-24599

[33] Leuthold J, Koos C, Freude W. Nonlinear silicon photonics. Nature Photon. 2010;**4**(8):35-544

[34] Driscoll JB, Astar W, Liu X, Dadap JI, Green WM, Vlasov YA, et al. All-optical wavelength conversion of 10 Gb/s RZ-OOK data in a silicon nanowire via cross-phase modulation: Experiment and theoretical investigation. IEEE Journal of Selected Topics in Quantum Electronics. 2010;**16**(5):1448-1459

[35] Xu QF, Lipson M. Carrier-induced optical bistability in silicon ring resonators. Optics Letters. 2006;**31**(3):341-343

[36] Khan M, Shen H, Xuan Y, Zhao L, Xiao S, Leaird DE, et al. Ultrabroad-bandwidth arbitrary radiofrequency waveform generation with a silicon photonic chip-based spectral shaper. Nature Photonics. 2010;**4**(2):117-122

[37] Zhang Y, Li DP, Zeng C, Huang ZZ, Wang Y, Huang QZ, et al. Silicon optical diode based on cascaded photonic crystal cavities. Optics Letters. 2014;**39**(6):1370-1373

[38] Bulgakov EN, Sadreev AF. All-optical diode based on dipole modes of Kerr microcavity in asymmetric L-shaped photonic crystal waveguide. Optics Letters. 2014;**39**(7):1787-1790

[39] Liu B, Liu YF, Jia C, He XD. All-optical diode structure based on asymmetrical coupling by a micro-cavity and FP cavity at two sides of photonic crystal waveguide. AIP Advances. 2016;**6**:065316